

**Measurements of positronium formation cross sections in positron-Mg collisions**

E. Surdutovich, M. Harte, W. E. Kauppila, C. K. Kwan, and T. S. Stein

*Department of Physics and Astronomy, Wayne State University, Detroit, Michigan 48202, USA*

(Received 30 January 2003; published 22 August 2003)

We report measurements of positronium (Ps) formation cross sections for 0.1–60 eV positrons scattered by Mg atoms. There is reasonable agreement between the measured cross sections and recent calculations of those values, both of which indicate an unusually steep increase of the Ps formation cross section from zero to a large peak value as the positron energy is increased from the Ps formation threshold to less than 1 eV above that threshold.

DOI: 10.1103/PhysRevA.68.022709

PACS number(s): 34.85.+x

**I. INTRODUCTION**

During the past decade our group has measured positronium (Ps) formation cross sections ( $Q_{Ps}$ 's) for positrons ( $e^+$ 's) scattered by hydrogen atoms, inert gases, alkali-metal atoms, and some molecules [1–5].  $Q_{Ps}$ 's have also been measured by other groups for  $e^+$ 's scattered by a variety of room-temperature gases and for atomic hydrogen [6]. These results, along with prior measurements of total cross sections ( $Q_T$ 's) for  $e^+$ 's scattered by the same target atoms and molecules [7], as well as corresponding calculated results indicate that the Ps formation channel plays an important role in  $e^+$  interactions with atoms and molecules at low to intermediate energies.

For the room-temperature gas atoms and molecules (such as  $H_2$ , He, Ne, Ar, Kr, Xe,  $N_2$ ,  $CO_2$ , etc.) there are generally pronounced increases in the  $Q_T$ 's when the  $e^+$  energy rises above the threshold for formation of Ps in its ground state [7]. For the alkali-metal atoms, due to their ionization threshold energies being less than the binding energy of Ps in its ground state (6.8 eV), Ps can be formed at arbitrarily low energies (“negative” Ps formation thresholds), and one does not see the effect of the Ps formation channel in the  $Q_T$ 's in an obvious way as in the case of the room-temperature gases. However, the role of Ps formation in  $e^+$ -alkali-metal-atom scattering is nonetheless important. For instance, it is remarkable that for some alkali metals, the neglect of the Ps formation channel in calculations related to  $e^+$ -alkali-metal-atom collisions leads to drastic disagreements between theory and experiment with the calculated  $Q_T$  results [8] being much *larger* than the corresponding measurements [9] at low energies, emphasizing the importance of taking the coupling between the Ps formation channel and other scattering channels into account in theoretical models.

Regarding our motivation for investigating Mg, we had pointed out sometime ago [10] that theoretical calculations [8,11] of  $Q_{Ps}$ 's for  $e^+$ -alkali-metal-atom collisions, with which our measured  $Q_{Ps}$ 's were in reasonable agreement, were consistent with a possible correlation between the relative proximities of the  $n=1$  or  $n=2$  Ps formation thresholds (“negative” or “positive”) to zero energy and the relative importance of the roles of those states in the overall Ps formation process. Consistent with this observation, Van Reeth *et al.* [12] have recently formulated a hypothesis, based on

existing calculated  $Q_{Ps}$  results [13] related to single ionization of the atom, that at a given incident  $e^+$  energy above the Ps formation threshold, the larger the difference  $E_r$  (whether positive or negative) between the kinetic energies of the incoming  $e^+$  and the outgoing Ps atom, the smaller is the Ps formation cross section. Van Reeth *et al.* show that a relationship of the form

$$Q_{Ps} = A \exp(-B|E_r|) \quad (1)$$

provides a quantitative description of the correlation between  $Q_{Ps}$  and  $E_r$ , described qualitatively above, where the positive coefficients  $A$  and  $B$  are energy-dependent parameters, one set of which would apply to all the inert gases, another set of which would apply to the ground ( $n=1$ ) states of all the alkali-metal atoms, and yet another set would apply to the  $n=2$  states of all the alkali-metal atoms. It should be noted that for single ionization,  $E_r$  is just  $E_{Ps}$ , the Ps formation threshold of the atom. Our observations for the alkali-metal atoms referred to above [10] and the quantitative analysis by Van Reeth *et al.* suggest the possibility that Ps formation in  $e^+$  collisions with target atoms whose Ps formation threshold energy  $E_{Ps}$  is close to zero may look like a resonant process in the sense that it may have particularly large values of  $Q_{Ps}$  at energies just above the threshold. Van Reeth *et al.* [12] also mention that the slope of the fit to Eq. (1) becomes smaller (the parameter  $B$  decreases) as the excess energy of the incident positron increases, and that this corresponds to the peak of  $Q_{Ps}$  being closer to the Ps formation threshold for atoms whose  $E_{Ps}$  values are closer to zero, which appears to be consistent with what we have observed for the inert gas atoms [3] and with the calculated [13]  $Q_{Ps}$  results for  $n=1$  and for  $n=2$  Ps formation in  $e^+$ -alkali-metal atom collisions.

In light of the above discussion, Mg is an interesting candidate for a detailed investigation of  $Q_{Ps}$ , since the threshold for ground-state Ps formation for Mg is 0.84 eV, which is significantly closer to a zero-energy Ps formation threshold than for any other atoms or molecules, for which  $Q_{Ps}$ 's have been measured so far, including the ground or excited Ps states of any of the alkali-metal atoms. If the hypothesis by Van Reeth *et al.* [12] referred to above applies to other atoms, including Mg, this would suggest that there is a possibility that the  $Q_{Ps}$  values could be rather large for Mg above its Ps formation threshold, and that  $Q_{Ps}$  could rise to its peak

value unusually abruptly as the  $e^+$  energy is increased. In the same light, it could be tempting to investigate atoms such as Ti, Cr, and Zr, whose ground state Ps formation thresholds of 0.02,  $-0.04$ , and 0.04 eV, respectively, are even closer to zero. Unfortunately, each of these atoms requires relatively high temperatures ( $>1000^\circ\text{C}$ ) to obtain vapor pressures sufficient for measurable attenuation of the  $e^+$  beam. On the other hand, in the case of Mg, a scattering-cell temperature of about  $350^\circ\text{C}$  is sufficient for obtaining a measurable attenuation of the  $e^+$  beam.

Another motivation for studying Mg is that it is a member of the alkaline-earth metal family of elements that has never been investigated in an  $e^+$  scattering experiment.

## II. EXPERIMENTAL APPROACH

We carried out all the  $Q_{\text{Ps}}$  measurements on Mg using the same apparatus that we have used before for measuring  $Q_{\text{Ps}}$ 's in  $e^+$ -alkali-metal-atom scattering described in Refs. [2,4,5] except for a relatively minor modification. A description of the experiment follows.

Positrons emitted by a  $^{22}\text{Na}$  source are slowed by a set of three annealed tungsten meshes serving as a moderator, focused by an electrostatic lens system, and guided by an axial magnetic field to form a beam that passes through the scattering cell. The measured energy width of our  $e^+$  beam (full width at half maximum) is energy dependent and typically several tenths of an eV. The axial magnetic field in the scattering cell ( $\approx 90$  G) is large enough to prevent  $e^+$ 's, which scatter elastically or inelastically without forming Ps, from reaching the walls of the scattering cell. The stainless steel scattering cell is an oven with an attached cylinder that serves as a reservoir for the metal whose atoms we wish to use as target atoms for  $e^+$  collisions. When the cell is at a relatively low temperature ("cold"),  $e^+$ 's pass through it without significant attenuation and reach the channeltron electron multiplier (CEM) located just beyond the cell, enabling us to measure the primary beam counts. When the cell is heated sufficiently (by passing electric current through separate tantalum wire heating elements embedded in its walls and in the wall of its attached cylinder),  $e^+$ 's scatter from Mg atoms in the resulting vapor that fills the cell, and Ps is produced when the  $e^+$  energy is above the Ps formation threshold.

The energy of the  $e^+$  beam as it passes through the scattering cell is defined by the potential difference applied between the tungsten mesh moderator and the cell, and by the relative work functions of their respective surfaces. With the cell being cold and the potential difference between the moderator and ground set at a given value, the mean  $e^+$  beam energy can be measured using a retarding potential technique by varying the potential difference between the cell (which is electrically floating) and ground, and plotting the derivative of the resulting retarding potential curve with respect to the applied cell potential, which results in a bell-shaped curve. The position of the peak of this curve indicates the midpoint of the retarding curve falloff and hence, the mean energy of the  $e^+$  beam when the cell potential is set at zero. The width of the peak gives an indication of a combination of the en-

ergy width and the angular spread of the  $e^+$  beam. Using the cell retarding potential curve information, the potential applied to the cell can then be varied by an appropriate amount to set the actual  $e^+$  beam energy in the scattering cell at any desired value.

We measure upper limits ( $Q_{\text{UL}}$ 's) on  $Q_{\text{Ps}}$ , by measuring the attenuation of our  $e^+$  beam with the angular discrimination of our experiment deliberately made as poor as possible in order to keep scattered  $e^+$ 's (which have not formed Ps or annihilated otherwise) in the beam that exits the scattering cell with the unscattered  $e^+$ 's. This is accomplished by using the relatively large (90 G) axial magnetic field referred to above and a relatively large scattering-cell-exit aperture (4.76 mm inside diameter) compared to the entrance aperture (3.18 mm i.d.). Under these conditions, Ps formation can be the main contribution to the attenuation of the  $e^+$  beam over a significant energy range above the Ps formation threshold. We then obtain  $Q_{\text{UL}}$  from the relationship

$$\mathcal{I} = \mathcal{I}_0 \exp(-nQ_{\text{UL}}L), \quad (2)$$

where  $\mathcal{I}_0$  is the transmitted beam count rate with the scattering cell "cold" (no appreciable vapor pressure in the cell),  $\mathcal{I}$  is the transmitted beam count rate with the cell "hot" (Mg vapor of number density  $n$  in the cell), and  $L$  is the path length of the beam through the cell (essentially the distance between the entrance and exit apertures of the cell). The number density is obtained by measuring the temperature of the scattering cell and using published vapor pressure data [14] along with the ideal-gas law. The "cross section"  $Q_{\text{UL}}$  obtained in this way is regarded as an upper limit on the actual  $Q_{\text{Ps}}$  value because the  $e^+$  beam attenuation associated with this cross section is related not only to  $e^+$ 's that have formed Ps, but also to  $e^+$ 's that have been scattered into the backward hemisphere or at sufficiently large forward angles so that they are removed from the primary beam.

One-fourth of the Ps formed in the scattering cell is *para*-Ps (spin 0, mean lifetime 0.125 ns), while three-fourths is *ortho*-Ps (spin 1, mean lifetime 142 ns). The scattering cell has a square cross section and its walls are 1.27 cm apart. A free 1-eV *para*-Ps would travel about 0.05 mm prior to decaying into two back-to-back 511-keV  $\gamma$  rays, so even *para*-Ps with kinetic energy of the order of 100 eV moves only about 0.5 mm and will not even come close to reaching the inner surface of the scattering cell prior to annihilation. On the other hand, a free 1-eV *ortho*-Ps would travel about 6 cm prior to decaying into three  $\gamma$  rays with a total energy of 1022 keV, so if the Ps work function (or the "Ps formation potential") of the cell's coated inner surface is ignored, even a 0.1-eV *ortho*-Ps moving within  $70^\circ$  of being perpendicular to the cell wall would tend to strike the wall before annihilating in flight. However, a negative Ps work function of the cell's coated surface of the order of 1 eV would imply that *ortho*-Ps with less than that amount of kinetic energy would not tend to strike the oven surface, so the Ps work function of the scattering-cell surface could play an important role in these considerations for low-energy *ortho*-Ps. For the *ortho*-Ps's that do reach the inner surface of the scattering cell, their interaction with the surface could give rise to the pro-

duction of two 511-keV  $\gamma$  rays by conversion into *para*-Ps or a breakup (if the *ortho*-Ps has sufficient kinetic energy) into an  $e^+$  and an  $e^-$  with the subsequent annihilation of the  $e^+$  with an  $e^-$  in the surface. Thus, by detecting coincidences of  $2\gamma$  rays within appropriate energy windows (set to  $511 \pm 50$  keV) using two photomultiplier tubes with attached NaI(Tl) scintillators located on opposite sides of the scattering cell, we can place a lower limit,  $Q_{LL}$  on  $Q_{Ps}$ , because the measured  $2\gamma$  signal can account for all of the *para*-Ps and a significant fraction of the *ortho*-Ps that is formed in our cell. We determine the overall detection efficiency of our system for the  $2\gamma$  signal using a calibrated sodium 22 source.

We also detect coincidences of two out of the three  $\gamma$  ( $2/3\gamma$ ) rays coming from decays of *ortho*-Ps in flight by setting energy windows between 300 and 460 keV. Although the overall detection efficiency of our system for this signal is not easy to determine, we have been exploring different ways to measure it, and by doing so, we are learning more about the amount of *ortho*-Ps that decays in flight. We call the corresponding measured cross section  $Q_{2/3\gamma}$ . We can obtain actual  $Q_{Ps}$  values by adding contributions that come from  $2\gamma$  and  $2/3\gamma$  coincidence signals once the overall detection efficiency of our system for the  $2/3\gamma$  signal has been determined.

As explained in Ref. [5], we use an iterative procedure to obtain our measured  $Q_{LL}$  values, starting with the formula

$$Q_{LL}^{(1)} = \frac{Q_T N_{2\gamma} \epsilon_{CEM}}{N_0 e^{-nQ_T L_a} (1 - e^{-nQ_T D}) \epsilon_{2\gamma} F_\gamma^2}, \quad (3)$$

where  $N_{2\gamma}$  is the rate of  $2\gamma$  coincidences,  $N_0$  is the rate of  $e^+$  counts in the unattenuated (cold) primary beam,  $n$  is the Mg atom number density in the vapor that fills the cell,  $\epsilon_{CEM}$  is the channeltron efficiency for  $e^+$  detection,  $\epsilon_{2\gamma}$  is the  $2\gamma$  coincidence detection efficiency,  $F_\gamma$  is the transmission coefficient of 511-keV  $\gamma$  rays by the cell's walls,  $L_a$  is the beam path length from the entrance aperture of the cell to the front edges of the scintillators, and  $D$  is the beam path length between the scintillators. The actual  $Q_{LL}$  values are then obtained by iteratively using the formula

$$Q_{LL}^{(i+1)} = \frac{Q_{LL}^{(i)} N_{2\gamma} \epsilon_{CEM}}{N_0 e^{-nQ_{LL}^{(i)} L_a} (1 - e^{-nQ_{LL}^{(i)} D}) \epsilon_{2\gamma} F_\gamma^2}, \quad (4)$$

and starting with  $Q_{LL}^{(1)}$  obtained from Eq. (3) in the limit where  $Q_T$  goes to zero, as explained in Ref. [5]. The iteration procedure does not depend on  $Q_T$  and it converges in essentially all cases within five iterations. The resulting  $Q_{LL}$  is based only upon the  $2\gamma$  signal that we measure.

The ‘‘two of three’’  $\gamma$  cross section  $Q_{2/3\gamma}$  should be calculated using a formula similar to Eq. (4) with  $N_{2\gamma}$  replaced by the rate of  $2/3\gamma$  coincidences,  $N_{2/3\gamma}$ , and  $Q_{LL}^{(i)}$  on the right-hand side replaced by  $Q_{LL} + Q_{2/3\gamma}^{(i)}$  (since both the  $2\gamma$  and  $2/3\gamma$  signals are related to Ps formation and as such are both connected to the attenuation of the  $e^+$  beam),  $\epsilon_{2\gamma}$  replaced by  $\epsilon_{2/3\gamma}$  (the  $2/3\gamma$  detection efficiency which we do not yet know), and where  $F_\gamma$  in this case is the transmission

coefficient of the  $\gamma$  rays that contribute to our  $2/3\gamma$  signal (which would be expected to be lower than the corresponding coefficient for the 511-keV  $\gamma$  rays).

If we are able to determine  $\epsilon_{2/3\gamma}$  to our satisfaction, we will then be able to obtain the iterated value of  $Q_{2/3\gamma}$ , add it to  $Q_{LL}^{(i)}$  on the right-hand side of Eq. (4) to include the attenuation of the  $e^+$  beam due to the  $2/3\gamma$  signal in the lower limit, and then continue substitutions of the converging values of  $Q$ 's until both  $Q_{LL}$  and  $Q_{2/3\gamma}$  converge. Then the sum of these converged cross sections would correspond to the ‘‘total Ps formation cross section,’’  $Q_{Ps}$ .

In this work a value of  $Q_{2/3\gamma}$  is determined as just described, but using the same product  $\epsilon_{2\gamma} F_\gamma^2$  (instead of  $\epsilon_{2/3\gamma} F_\gamma^2$ ) in the denominator of Eq. (4) as for the  $2\gamma$  signal. Preliminary evidence is provided below that doing this may be a reasonable starting point for our present stage of accuracy of our  $Q_{Ps}$  measurements.

Using Eq. (4) to determine  $Q_{LL}$  in the absence of knowledge of  $\epsilon_{2/3\gamma}$ , we assume that the attenuation of the beam is due to the  $2\gamma$  signal alone so the corresponding cross section  $Q_{LL}$  maintains its status of a valid lower limit.

The first step in measuring a set of cross sections ( $Q_{UL}$ ,  $Q_{LL}$ , and  $Q_{2/3\gamma}$ ) is to adjust the  $e^+$  beam tuning parameters (lens voltages and magnetic-field coil currents) in the system to optimize transmission of the  $e^+$  beam with the scattering-cell cold for a given  $e^+$  beam energy. Normally, our  $Q_{UL}$ ,  $Q_{LL}$ , and  $Q_{2/3\gamma}$  measurements are based upon a so-called ‘‘hot run’’ (scattering-cell temperature high enough to significantly attenuate the  $e^+$  beam) bracketed by two ‘‘cold runs’’ (scattering-cell temperature low enough to cause no significant attenuation of the  $e^+$  beam) for each  $e^+$  beam energy. Then this sequence of events is repeated for each new  $e^+$  beam energy that we wish to investigate. Reasonable agreement of the cold runs before and after a given hot run is required for the data from such a sequence of measurements to be considered reliable.

For our  $Q_{UL}$  and  $Q_{LL}$  measurements, we have also performed energy scans by optimizing the tuning of the  $e^+$  beam with the scattering cell cold for an energy located in the scanned energy range and then increasing the scattering-cell temperature for the hot run and simply stepping the cell voltage along by discrete increments and measuring coincidence count rates and the transmitted  $e^+$  beam count rates at each of those energies with the cell maintained at the high temperature before making the final cold run. This enables us to obtain much more data in a given period of time because we can avoid cycling the temperature from cold to hot to cold (a very time-consuming procedure) for each separate energy value that we wish to investigate.

Regarding the ‘‘minor modification’’ in apparatus mentioned at the beginning of this section, one of the major challenges we encountered in trying to measure  $Q_{Ps}$  for Mg with our heated scattering cell was related to the need to establish a reasonably uniform coating of the Mg on the inner surfaces of that cell. The scattering apparatus used in this experiment was originally designed for investigations of the alkali-metal atoms. Our work with the alkali-metal atoms had indicated that it was important to precoat the scattering-

cell walls with the alkali metal being investigated and to maintain a reasonably uniform coating during the data runs in order to obtain reliable estimates of vapor pressures based upon measurements of cell-wall temperatures. When the cylinder which served as a reservoir for the alkali metals was heated, the alkali metal would melt and the vapor that was produced would condense on the inner surfaces of the scattering cell and wet and eventually visibly coat those surfaces. Since the scattering cell is heated as well, there is a dynamic equilibrium between these coated surfaces and the vapor in the cell (we try to compensate for the loss of atoms due to effusion from the entrance and exit apertures of the cell by maintaining the cylinder at a slightly higher temperature than the scattering cell). We believe that it is reasonable under these conditions to make use of published saturation vapor pressure data [14] along with measured cell-wall temperatures and the ideal-gas law to determine the number density of atoms in the scattering cell.

Magnesium does not melt when heated, but rather it sublimates, resulting in vapor that condenses on some parts of the cell walls, but it does not wet the cell walls and we found that it was considerably more difficult to obtain a reasonably uniform Mg coating on all the inner cell-wall surfaces. As a result, we were plagued for an extended period of time with unreproducible cross-section results. We ended up dealing with this problem by inserting a cylindrical tube machined from solid Mg that fits snugly inside the scattering cell. The internal surface of this tube served as our Mg lining for our scattering cell rather than relying upon the particularly non-uniform coating produced by migration of atoms from the cylindrical reservoir to the scattering cell above it. We also machined slots in the bottom part of the Mg tube so that Mg vapor originating from the Mg ribbon in our heated cylindrical reservoir could enter the interior of the Mg tube and “refresh” the inner surface of that tube during our data runs.

Another difficulty that arose was that after making cross-section measurements with Mg for a few days, an excessive buildup of the metal would tend to occur in certain locations inside of our scattering cell, in apertures, and in other parts of the system and that would reduce the transmission of our  $e^+$  beam through our system to the CEM detector. This resulted in more  $e^+$ 's entering the scattering cell than reaching the detector, and a corresponding undercounting of the primary  $e^+$  beam, which would tend to make  $Q_{LL}$  and  $Q_{2/3\gamma}$  values too high. The excessive buildup of Mg can also narrow the exit aperture of the scattering cell and the aperture of a retarding element following the scattering cell, and narrower apertures could provide better angular discrimination which could make  $Q_{UL}$  too high also. On the other hand, if the Mg coating became nonuniform, or was oxidized or contaminated in some other way, and no longer was adequate for producing the expected equilibrium vapor pressure for Mg corresponding to a given cell-wall temperature, our measured  $Q_{UL}$ ,  $Q_{LL}$ , and  $Q_{2/3\gamma}$  values could tend to be too low.

Since  $Q_{UL}$  involves a relative measurement (the ratio of the attenuated to unattenuated beam count rates), it is fairly insensitive to many problems that can plague our absolute coincidence measurements ( $Q_{LL}$ ,  $Q_{2/3\gamma}$ ), but it would still tend to be sensitive to the problems referred to above such as

the development of nonuniform Mg coatings, contamination of the Mg coatings, or the buildup of excessive Mg deposits. When our measured  $Q_{UL}$  curves were carefully monitored over time, significant changes in absolute  $Q_{UL}$  values or in the shape of the  $Q_{UL}$  curve helped make us aware that such problems could be occurring and gave us a basis for rejecting unreliable data.

An additional check on whether our cross-section measurements were making sense was provided by whether  $Q_{LL}$  was approaching zero when the  $e^+$  beam energy was reduced below  $E_{Ps}$  allowing for the energy width of the beam. When problems were developing with uneven or contaminated coatings or excessive buildups of Mg, we could easily undercount the primary beam due to not having all the beam that enters the scattering cell reach the CEM detector because of blockages by the Mg buildups or due to deflection of the beam related to asymmetries or other changes in the Mg coating. This would result in our measured cross sections being too high and this problem could be particularly severe as the  $e^+$  beam energy approached low energies ( $<2$  eV) regardless of the 0.84-eV threshold of Ps formation. Thus, indications of rising values of our measured cross sections at the lowest energies, rather than the expected decrease in their values as the positron energy was approaching close to the Ps formation threshold, served to warn us that problems were arising and provided an additional criterion for rejecting unreliable data.

It should also be noted that every time measurements for a given  $e^+$  beam energy are made, the temperature of the scattering cell and the corresponding number density has been somewhat different, and since measured cross sections should be independent of number density, this provides an ongoing check of internal consistency of our data as we go back and remeasure cross sections for given energies to test for repeatability of our results. For the data that we deem reliable, there are no indications of dependence of our measured cross sections on number density.

### III. RESULTS AND DISCUSSION

The tabulated averaged results of the lower limits ( $Q_{LL}$ ) and the upper limits ( $Q_{UL}$ ) on  $Q_{Ps}$  are given in Table I and are plotted versus  $e^+$  energy in Fig. 1 along with  $Q_{Ps}$ 's calculated by Walters [15] using a coupled-state approximation and by Hewitt *et al.* using a close-coupling approximation [16], and also inelastic cross sections obtained by Gribakin and King [17] using an *ab initio* many-body correlation potential calculation which should represent  $Q_{Ps}$  up to the threshold (4.3 eV) for excitation of Mg by  $e^+$ 's. Our measured upper limits and lower limits, taking their respective error bars and the energy width of our  $e^+$  beam into account, essentially bracket (and therefore are consistent with) all of the theoretical calculations shown in Fig. 1. Our measured upper limits are reasonably close to the calculated results of Walters up to about 20 eV, shapewise and absolute-value-wise. The energy dependence of our measured  $Q_{LL}$ 's appears to be consistent with the calculated Ps formation threshold (0.84 eV). Our  $Q_{LL}$  values fall off as the  $e^+$  energy is reduced below 1.1 eV,  $Q_{LL}$  is essentially zero at about 0.12 eV,

TABLE I. Positronium formation cross sections in  $e^+$ -Mg scattering: lower and upper limits with statistical uncertainties (in parentheses) with respect to  $e^+$  energy.

Energy (eV)	Lower limit ( $\text{\AA}^2$ )	Energy (eV)	Upper limit ( $\text{\AA}^2$ )
0.12	1.4(0.3)	1.2	74.0(0.5)
0.6	13.4(0.3)	2.0	68.5(0.2)
1.1	22.7(0.3)	4.0	50.4(0.4)
2.0	22.6(0.3)	6.0	40.6(0.1)
4.0	17.9(0.2)	8.0	32.7(0.1)
6.1	16.4(0.2)	9.9	26.7(0.4)
8.1	10.7(0.2)	15.0	20.6(0.1)
10.1	10.6(0.2)	20.0	15.7(0.1)
15.0	5.9(0.3)	25.0	15.9(0.1)
20.0	5.4(0.2)	30.0	10.7(0.2)
25.0	3.6(0.3)	40.0	10.8(0.2)
30.0	2.5(0.1)	50.0	6.1(0.2)
40.0	2.0(0.1)	60.0	7.3(0.2)
50.1	1.2(0.1)		
60.1	0.9(0.1)		

and the value of  $13.4 \text{\AA}^2$  at 0.6 eV is sensible when the measured energy width of 0.4 eV at this energy for our  $e^+$  beam is taken into account.

If the energy width in our experiment were smaller, it would be tempting to look for evidence of increased annihilation  $\gamma$ -ray production below the energy threshold for Ps formation in Mg beyond what one would expect from free annihilation of the positron with an electron due to a predicted bound state that an  $e^+$  may form with Mg with a binding energy of  $\approx 0.9$  eV [18].

The position of the maximum in  $Q_{LL}$  also appears to be

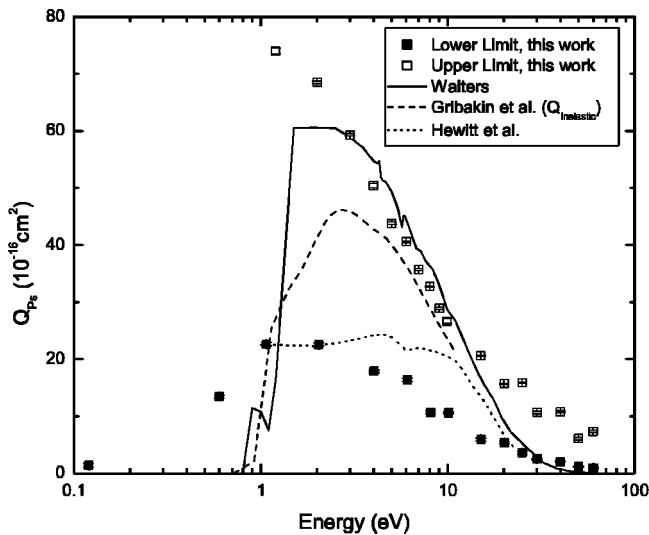


FIG. 1. Positronium formation cross sections in  $e^+$ -Mg scattering: lower and upper limits are shown (error bars in this and the following figures represent statistical uncertainties, except where error bars are encompassed by the size of the symbols) and compared with theoretical results by Walters [15], Gribakin and King [17] (inelastic cross sections), and Hewitt *et al.* [16].

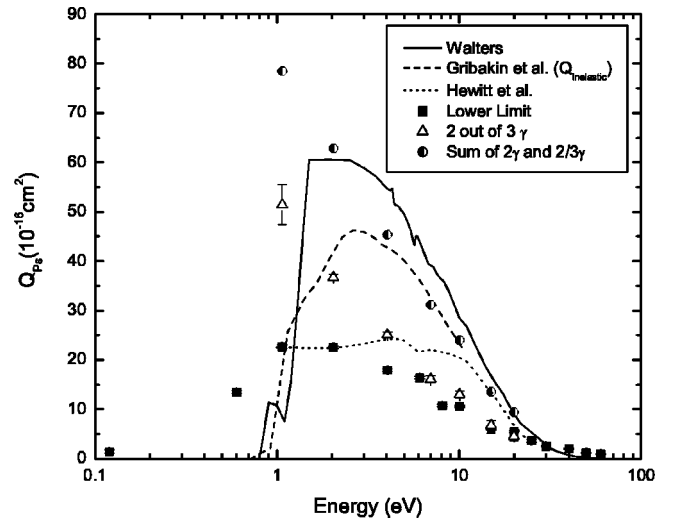


FIG. 2. Lower limit is shown along with  $Q_{2/3\gamma}$  and  $Q_{2\gamma} + Q_{2/3\gamma}$ ; they are compared to the theoretical results by Walters [15], Gribakin and King [17], and Hewitt *et al.* [16].

consistent with the calculations of Walters, indicating that  $Q_{Ps}$  rises from zero at threshold to its maximum when the  $e^+$  beam energy has been increased by less than 1 eV, which represents a much steeper rise of  $Q_{Ps}$  to its maximum than for any other target atom or molecule that has been investigated up to the present time. This is intriguing in view of the discussion in Sec. I of this paper, which suggests that a steep rise to a maximum may be consistent with having a Ps formation energy threshold near zero energy, which is the case for Mg.

The  $Q_{2/3\gamma}$  results obtained using the same product  $\epsilon_{2\gamma}F_{\gamma}^2$  of detection sensitivity and the square of the  $\gamma$  transmission coefficient in the denominator of Eq. (4) as for the  $2\gamma$  signal are shown in Fig. 2 along with the  $Q_{LL}$  values and the theoretical results [15–17] that were shown in Fig. 1. The sum of the *iterated* lower limit (which we call  $Q_{2\gamma}$ ) and  $Q_{2/3\gamma}$  is also plotted in Fig. 2. If the product  $\epsilon_{2\gamma}F_{\gamma}^2$  that pertains to the  $\gamma$ -ray signal resulting from decay of *ortho*-Ps in flight were known, this sum would be the actual Ps formation cross section,  $Q_{Ps}$ . However, there are some indications that the procedure we are presently following to obtain our  $Q_{2/3\gamma}$  results may be a reasonable starting approximation to the cross section that represents the *ortho*-Ps formed in our system that decays in flight. The argument for this follows.

If the  $e^+$  beam energy is set so that it is just barely above  $E_{Ps}$ , then the resulting Ps's will have very little kinetic energy. In the limiting case as the  $e^+$  beam energy approaches  $E_{Ps}$ , the *ortho*-Ps is moving so slowly that it cannot reach the walls of the scattering cell and would be guaranteed to decay in flight. In such a case, since there is three times as much *ortho*-Ps as *para*-Ps formed in the scattering cell, one might expect the ratio of  $Q_{2/3\gamma}$  to  $Q_{2\gamma}$  to approach 3:1. However, a more careful analysis of a Dalitz plot [19] for  $3\gamma$  decay, taking the widths of our energy windows for detecting the  $\gamma$  rays associated with  $2\gamma$  and  $3\gamma$  decays into account, suggests that this ratio should actually be about 1.5.

In Fig. 3, the ratio of  $Q_{2/3\gamma}$  to  $Q_{2\gamma}$  is plotted versus  $e^+$

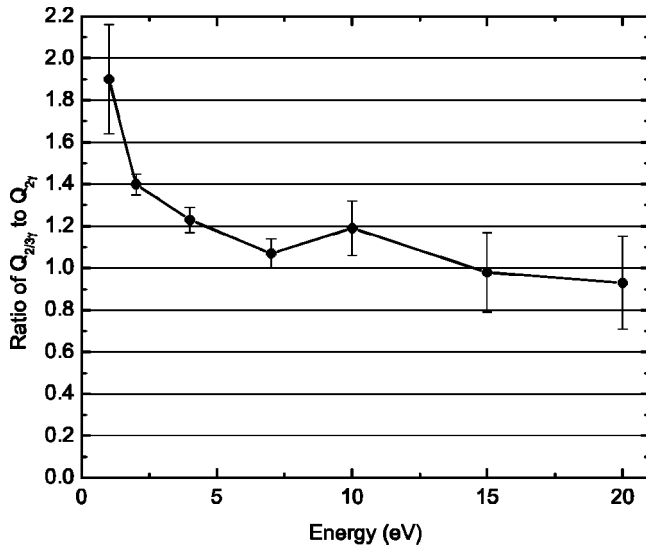


FIG. 3. The ratio of  $Q_{2\beta\gamma}$  to  $Q_{2\gamma}$  with respect to  $e^+$  energy.

beam energy. We believe that there could be some interesting physics related to the interaction of *ortho*-Ps with surfaces revealed by such a plot. The ratio increases as the  $e^+$  energy is reduced from a value of about 1 (above 7 eV) and reaches a value of  $1.9 \pm 0.3$  near 1 eV, the lowest energy at which the ratio was measured. It is encouraging that the ratio decreases as the  $e^+$  energy is increased, since we would expect that as the *ortho*-Ps energy is increased, its tendency to interact with the wall and to give rise to a  $2\gamma$  coincidence signal would increase, thus increasing the signal that contributes to  $Q_{2\gamma}$  and decreasing the amount of *ortho*-Ps that decays in flight and correspondingly the  $Q_{2\beta\gamma}$  value. The measured ratio at 1 eV is nearly within its uncertainty of the estimated value of 1.5 discussed above. This indicates that our use of the same product  $\epsilon_{2\gamma}F_{\gamma}^2$  in calculating  $Q_{2\beta\gamma}$  as for calculating  $Q_{LL}$  may be a reasonable rough starting approximation given the present uncertainties of our measurements.

It is also worthwhile noting that our measured ratio of  $Q_{2\beta\gamma}$  to  $Q_{2\gamma}$  that we have recently reported [5] for Li is  $\approx 0.7$  and for Na is about 0.5 for all energies investigated. We find the apparent differences between the ratios for Li, Na, and Mg curious. First, consider the general shape of the ratio curves. At higher energies for Mg and for all energies investigated for Li and Na [5] the ratios appear to be relatively independent of the  $e^+$  beam energy. A possible explanation for this is that when the  $e^+$  beam energy is a few eV or more above the Ps formation threshold, the *ortho*-Ps has sufficient energy to reach and interact with the coating on the cell wall and to break up. Since calculated Ps formation potentials [20] sometimes referred to as Ps work functions for some common metals such as Al, Cu, and Ni are between  $-2$  and  $-3$  eV, *ortho*-Ps with a few eV of kinetic energy approaching such a surface could possibly break up upon impact into an  $e^+$  and an  $e^-$ . The  $e^+$  has a reasonably high probability (can be greater than 50% for some elements) [20] of being reemitted as low energy Ps. If the  $e^+$  energy is larger than a few eV, this probability of reemission as Ps

appears to be relatively insensitive to the incident  $e^+$  energy within an  $e^+$  energy range of 100 eV or so. This could be consistent with the relatively energy-independent behavior of the ratio plotted for Mg in Fig. 3 when the  $e^+$  energy is a few eV or more above  $E_{Ps}$ . It could also be consistent with the relative energy independence of the Li and Na results discussed above over the whole energy range investigated if the Ps formation potential for those elements is of the order of those for the common metals, Al, Cu, and Ni (i.e., a few eV). The reason for this could be that the Ps formation thresholds for alkali-metal atoms are negative so the kinetic energies of the Ps formed in its ground state in collisions with the alkali-metal atoms can never be less than a few eV and so even for arbitrarily small incident  $e^+$  energy would be like the case for Mg when the incident  $e^+$  energy is a few eV or more. Comparing the ratios for Li (0.7) and Na (0.5) to that of Mg (1.0) at energies more than a few eV above  $E_{Ps}$  suggests that Na has the highest probability of conversion of the *ortho*-Ps into a  $2\gamma$  signal on the inner walls of the coated scattering cell while Mg has the lowest probability of conversion. It is interesting that this conversion probability appears to reach somewhat of a plateau at higher Ps energies that is characteristic of the particular substance being investigated.

The systematic errors in similar experiments were discussed in detail in Refs. [5,21]. The systematic uncertainties caused by spiraling trajectories of  $e^+$  and stray magnetic fields around the beam discussed in these references do not change in the case of Mg. They do not significantly contribute to the total systematic uncertainty. The main factor in the case of Mg is rather the quality of the Mg coating on the cell walls (uniformity and degree of contamination) and how this affects our determination of the number density of Mg atoms when we use Ref. [14]. Our estimates coming from the standard deviation of the upper limits are that the systematic errors caused by vapor density uncertainty may be about 20% of the measured  $Q_{Ps}$  at energies  $< 15$  eV and up to 40% at energies  $> 15$  eV.

We are in the process of trying to more accurately determine the appropriate product  $\epsilon_{2\beta\gamma}F_{\gamma}^2$  that should be used for our  $Q_{2\beta\gamma}$  data by investigating room-temperature gases. Our calculation of  $Q_{2\beta\gamma}$  and iteration of  $Q_{LL}$  to calculate  $Q_{2\gamma}$  involve the product that is used for the  $2\gamma$  signal instead of the unknown  $\epsilon_{2\beta\gamma}F_{\gamma}^2$ , but we consider this to be the best that we can do at this point to give an experimental indication of the actual value of  $Q_{Ps}$  for Mg. It is interesting that the resulting sum  $Q_{2\gamma} + Q_{2\beta\gamma}$  agrees reasonably well with the general shape of the calculations of  $Q_{Ps}$  and that our measured  $Q_{Ps}$ 's along with the calculated values suggest that  $Q_{Ps}$  rises steeply as the  $e^+$  beam energy is increased above  $E_{Ps}$  from zero to a large value within less than 1 eV above  $E_{Ps}$ .

#### ACKNOWLEDGMENTS

We would like to acknowledge H.R.J. Walters for helpful communications and the support by NSF Grant No. PHY99-88093.

- [1] S. Zhou, H. Li, W.E. Kauppila, C.K. Kwan, and T.S. Stein, *Phys. Rev. A* **55**, 361 (1997).
- [2] S. Zhou, S.P. Parikh, W.E. Kauppila, C.K. Kwan, D. Lin, A. Surdutovich, and T.S. Stein, *Phys. Rev. Lett.* **73**, 236 (1994).
- [3] K. Pipinos, M. S. thesis, Wayne State University, Detroit, Michigan, 2000 (unpublished).
- [4] A. Surdutovich, J. Jiang, W.E. Kauppila, C.K. Kwan, T.S. Stein, and S. Zhou, *Phys. Rev. A* **53**, 2861 (1996).
- [5] E. Surdutovich, J.M. Johnson, W.E. Kauppila, C.K. Kwan, and T.S. Stein, *Phys. Rev. A* **65**, 032713 (2002).
- [6] G. Laricchia and M. Charlton, in *Positron Beams and their Applications*, edited by P. Coleman (World Scientific, Singapore, 2000), p. 41.
- [7] W.E. Kauppila and T.S. Stein, *Adv. At., Mol., Opt. Phys.* **26**, 1 (1990).
- [8] R.N. Hewitt, C.J. Noble, and B.H. Bransden, *J. Phys. B* **26**, 3661 (1993).
- [9] S.P. Parikh, W.E. Kauppila, C.K. Kwan, R.A. Lukaszew, D. Przybyla, T.S. Stein, and S. Zhou, *Phys. Rev. A* **47**, 1535 (1993).
- [10] T.S. Stein, J. Jiang, W.E. Kauppila, C.K. Kwan, H. Li, A. Surdutovich, and S. Zhou, *Can. J. Phys.* **74**, 313 (1996).
- [11] A.A. Kernoghan, M.T. McAlinden, and H.R.J. Walters, *J. Phys. B* **29**, 3971 (1996).
- [12] P. Van Reeth, J.W. Humberston, G. Laricchia, and J.T. Dunn, *J. Phys. B* **33**, L669 (2000).
- [13] C.P. Campbell, M.T. McAlinden, A.A. Kernoghan, and H.R.J. Walters, *Nucl. Instrum. Methods Phys. Res. B* **143**, 41 (1998).
- [14] R.E. Honig and D.A. Kramer, *RCA Rev.* **30**, 285 (1969).
- [15] H. R. J. Walters (private communications).
- [16] R.N. Hewitt, C.J. Noble, B.H. Bransden, and C.J. Joachain, *Can. J. Phys.* **74**, 559 (1996).
- [17] G.F. Gribakin and W.A. King, *Can. J. Phys.* **74**, 449 (1996).
- [18] V.A. Dzuba, V.V. Flambaum, G.F. Gribakin, and W.A. King, *Phys. Rev. A* **52**, 4541 (1995).
- [19] R.H. Dalitz, *Philos. Mag.* **44**, 1068 (1953).
- [20] P.J. Schultz and K.G. Lynn, *Rev. Mod. Phys.* **60**, 701 (1988).
- [21] C.K. Kwan, W.E. Kauppila, R.A. Lukaszew, S.P. Parikh, T.S. Stein, Y.J. Wan, and M.S. Dababneh, *Phys. Rev. A* **44**, 1620 (1991).